MATTER: International Journal of Science and Technology
ISSN 2454-5880

Tamkuan & Nagai, 2019

Volume 5 Issue 1, pp. 23-35

Date of Publication: 6th April 2019

DOI-https://dx.doi.org/10.20319/mijst.2019.51.2335

This paper can be cited as: Tamkuan, N. & Nagai, M. (2019). Sentınel-1A Analysıs for Damage Assessment: A Case Study of Kumamoto Earthquake ın 2016. MATTER: International Journal of Science and Technology, 5(1), 23-35.

SENTINEL-1A ANALYSIS FOR DAMAGE ASSESSMENT: A CASE STUDY OF KUMAMOTO EARTHQUAKE IN 2016

Nopphawan Tamkuan
Graduate School of Sciences and Technology for Innovation, Yamaguchi University, 2-16-1, Tokiwadai, Ube, Yamaguchi 755-8611, Japan
nopphawan.yui@gmail.com

Masahiko Nagai
Graduate School of Sciences and Technology for Innovation, Yamaguchi University, 2-16-1, Tokiwadai, Ube, Yamaguchi 755-8611, Japan
nagaim@yamaguchi-u.ac.jp

Abstract

The powerful earthquakes occurred in Kumamoto at the highest magnitude 7.3 hitting this prefecture on April 16, 2016 at 01.25 A.M. local time. This study proposed a method to utilize Sentinel-1A images to detect earthquake damaged areas. There were two images being used. One was before-earthquake images (on March 3, 2016 and March, 27 2016) and another was an after-earthquake image (on April 20, 2016). The method operated on interferometric coherence of sentinel-1A image. In order to estimate the damaged areas, the coherence change between the before-earthquake and during-earthquake pairs were processed. The damage map was produced by concerning into different classes comprised of the urban damaged areas, none and less damaged of the urban areas, and non-urban areas. This approach was compared with the ground-truth data, which provides high overall accuracy at 88% (kappa coefficient is 0.82).

Consequently, Sentinel-1A could contribute the insightful geospatial information of the earthquake situation and support the disaster management.

Keywords

Damage Assessment, Sentinel-1A, Interferometric Coherence, Kumamoto Earthquake

1. Introduction

An earthquake is the most destructive natural hazard and it is difficult to predict exactly where and when it will happen. It can broadly cause significant damaging to buildings and other infrastructure. Therefore, the responded process after the disaster is an important task to reduce the diverse impacts on communities (Ansal, 2014). Currently, technology has become an important role for disaster management. An example of remote sensing technology (Yamazaki & Matsuoka, 2007) was applied in a post-disaster assessment. Also, another is a social networking service, such as twitter was beneficial for emergence response (M. Ventayen, 2017). A spatial information of disaster situation is critical information to support recovery, mitigation, and planning in disaster management (Eguchi et al., 2001; Miyazaki, Nagai, & Shibasaki, 2015). For instance, urban flood vulnerability mapping could help make a decision on flood disaster planning (Usman Kaoje & Ishiaku, 2017).

Synthetic Aperture Radar (SAR) system is one of remote sensing technology, which has been useful for disaster monitoring and damage evaluation in spatial and temporal dimensions. SAR could perform high capability for rapid observation because it is capable of cloud penetration without time limitation by performing both night and day time. SAR effectively provides rapid response for the disaster conditions. An instance of SAR, COSMO-Skymed could rapidly detect landslide using backscattering coefficient difference and intensity (Konishi & Suga, 2018). SAR interferometry is an advanced technique in remote sensing for geophysical monitoring. It has been widely used to detect and monitoring natural hazards related to the ground deformation such as the land subsidence (Ouchi, 2013) and earthquakes (Stramondo, Moro, Tolomei, Cinti, & Doumaz, 2005; Raucoules, Ristori, de Michele, & Briole, 2010).

Furthermore, multi-temporal SAR images have been utilized for damage assessment by analyzing the intensity correlation and interferometric coherence (Plank, 2014). These methods were usually implemented using at least two times of SAR data with pre and post-earthquake for detecting damaged areas (Matsuoka & Yamazaki, 2005) including of utilizing from several SAR sensors such as ALOS-2-PALSAR-2 (L-Band) with interferometric coherence change could also

be helpful to identify the damages of Gorkha earthquake, Nepal in 2015 (Watanabe et al., 2016). The difference of phase-corrected coherence between ALOS pre-seismic and co-seismic SAR data pairs were analyzed to discover the change of surface scattering properties caused by the 2011 Tohoku earthquake (Ishitsuka, Tsuji, & Matsuoka, 2013). ALOS-2 with interferometric coherence change could create the damage assessment map for Kumamoto earthquake in 2016 with reasonable accuracy (Tamkuan & Nagai, 2017).

Additionally, Sentinel-1A data is freely available to support various disaster applications (ESA, 2012) such as the automated flood detection and near-real-time monitoring (Twele, Cao, Plank, & Martinis, 2016). Multi-temporal series of Sentinel-1A measured the spatial autocorrelation change induced by landslide (Mondini, 2017). Interferometric synthetic aperture radar (InSAR) result of Seninel-1A provided the deformation information of earthquakes (Suresh & Yarrakula, 2018). Therefore, this study proposed a method to detect the affected areas for Kumamoto earthquake in 2016 using Sentinel-1A. GMTSAR (freely modified and redistribute) was also used for processing. The procedures and results of this study could support the disaster management and apply for unpredictable disaster in the future.

2. Study Area, Data and Software

2.1 Study Area

On April 14, 2016, the earthquake hit west central Kyushu region with foreshock 6.2 Mw. Two days later on April 16, the destructive main shock 7.0 Mw occurred again. These earthquakes resulted in 67 severe casualties, high number of injured (more than 1,600 people) and evacuated at the peak (more than 180,000 people). Moreover, plenty of buildings and other infrastructure facilities were damaged in the vast area (USGS, 2016).

2.2 Data Used and Software

All data is publicly available on the internet. ASTER GDEM (Global Digital Elevation Model) with 30 meters was used to correct the phase and removed the topography for detecting the interferogram of ground displacement. Sentinel-1A images were downloaded in Interferometric Wide (IW) swath mode derived from the Copernicus Open Access Hub (https://scihub.copernicus.eu/). This mode is a main acquisition mode of Sentinel-1A. It covers with 250 kilometers swath at 5 meters by 20 meters spatial resolution (single look). IW mode captures three sub-swaths using Terrain Observation with Progressive Scans SAR (TOPSAR). The products were taken from descending with level-1 images. The three Sentinel-

1A images on March 3, March 27, and April 20 in 2016 were operated in this study. The information of the images is shown as followings:

- S1A_IW_SLC__1SSV_20160303T211629_20160303T211657_010210_00F131_E721.SAFE
- S1A_IW_SLC__1SSV_20160327T211629_20160327T211657_010560_00FB2D_CC6B.SAFE
- S1A_IW_SLC__1SSV_20160420T211630_20160420T211658_010910_01059E_8779.SAFE

The study was processed by open source tools and free software. InSAR processing was done by GMTSAR which is written in C, compiled with GMT (Generic Mapping Tools) and NETCDF operating on Linux operating system (D. Sandwell et al., 2016). The license is open under a General Public License (GNU), it can be modified and redistributed. Plus, QGIS software (GNU license) was used for defining the threshold and classifying the damage map.

3. Methodology

3.1 Differential Interferometry Technique (DInSAR)

DInSAR is a geodetic technique to identify the surface movement and deformation by phase difference between two or more SAR images looking at the same scene from comparable geometries (Polcari et al., 2014). The interferogram could be calculated by GMTSAR (D. Sandwell et al., 2016; D. T. Sandwell, Mellors, Xiaopeng, Matt, & Wessel, 2011; D. Sandwell et al., 2011). As our study, we applied two pass method using an external digital elevation model (DEM) and converted into the interferogram phase, which subtracted from the SAR interferogram image for observing the surface deformation. First of all, the alignment was processed to register the images. Interfere is to generate interferogram by removing topographic phase using DEM. The filter/snaphu were computed the standard products. Finally, geocode was converted from radar coordinate to longitude-latitude system as the diagram shown in figure 1. The software creates an interferometric phase, coherence, unwrapped phase, and others. The coherence was used for the damage assessment in our study.

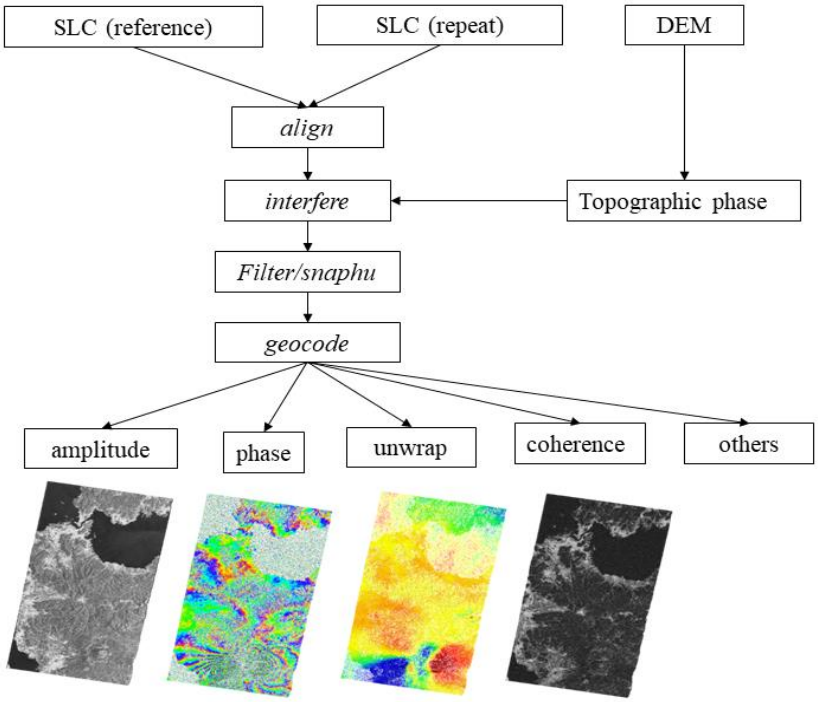

Figure 1: *The Diagram shows the Products of DInSAR, which Modified from GMTSAR (D. Sandwell et al., 2016)*

3.2 Interferometric Coherence Change and Damage Assessment

The coherence from DInSAR has been an advantage of examining the quality of interferogram and estimate the ground surface changes including of collapsed and damaged buildings. A pair of DInSAR can show a degree of coherence between two SAR images. Low coherence means high surface change between two acquisitions. Moreover, the comparison of the pre-disaster and co-disaster interferogram correlation could evaluate the change caused by earthquake (Hoffmann, 2007; Watanabe et al., 2016; Arciniegas, Bijker, Kerle, & Tolpekin, 2007). The coherence (Υ) was defined as a magnitude of the cross-correlation coefficient between two co-registered complex images as the equation (1):

$$\Upsilon = \frac{|\langle S_1 S_2^* \rangle|}{\sqrt{\langle S_1 S_1^* \rangle \langle S_2 S_2^* \rangle}} \qquad (1)$$

Where S1 and S1 are denoted as corresponding complexes of two single look complex. S* is complex conjugate of S. Its value could be from 0 to 1, which mean no-correlation and prefect correlation respectively.

The damage assessment map was investigated by three images of Sentinel-1A as shown in figure 2. Firstly, a pre-seismic and co-seismic coherence were performed by DInSAR technique. The pre-seismic coherence later identified the urban areas concerning the value greater than mean-3SD of ground truth. The portion in the urban areas, the pre-seismic and co-seismic coherence can be utilized for the damage assessment by applying the normalized differences (ND). It can be computed by equation 2. γ_{pre} and γ_{co} were represented the pre-earthquake SAR image pair, and pre- and co-earthquake image pair respectively.

$$ND = \frac{\gamma_{pre} - \gamma_{co}}{\gamma_{pre} + \gamma_{co}} \quad (2)$$

The high-level index presents a high level of surface physical changes due to the damaged areas. The areas were determined by the value, which is greater than mean-3SD of the known damaged area. The accuracy assessment was compared with ground-truth data using confusion matrix method.

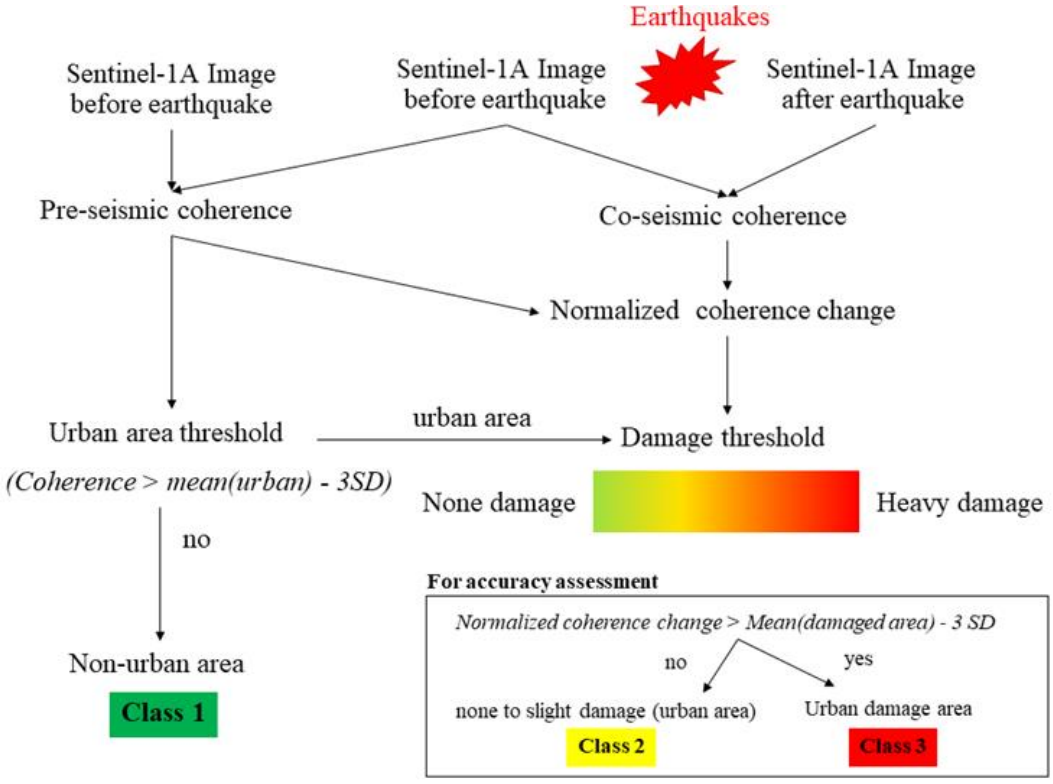

Figure 2: *Methodology of the Damage Assessment using Sentinel-1A Image*

3. Result and Discussion

DInSAR provides the achievement for detecting the Kumamoto earthquake deformation. The interferogram in figure 3 represented the co-seismic displacement (during March 27 to April 20, 2016) with many fringes. One fringe is between half of wavelength or -λ/2 (-2.8 cm) to + λ/2 (2.8 cm) displacement of C-band from the satellite look direction. The positive and negative value means the further and closer to the sensors. The abovementioned information could roughly imply the ground deformation and surface ruptures.

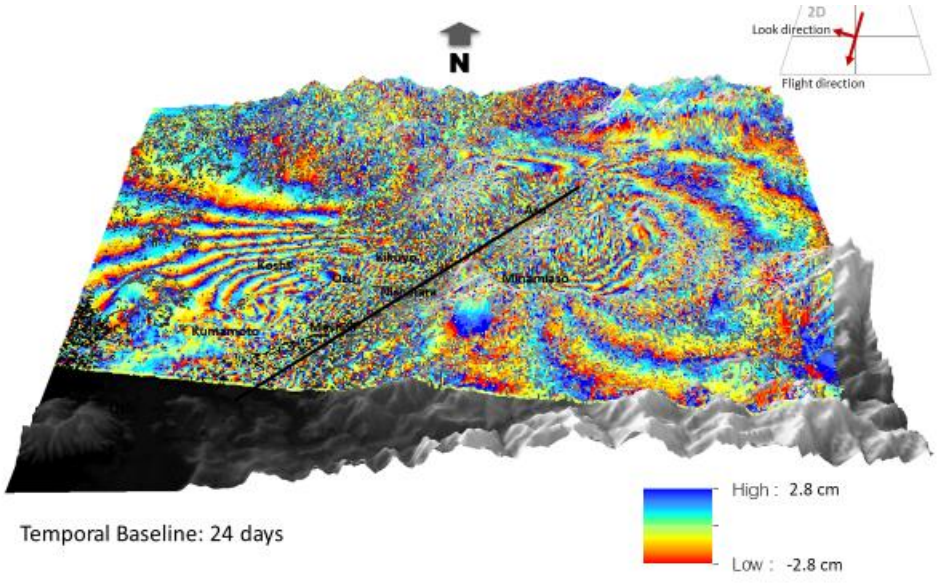

Figure 3: *Interferogram of Co-Seismic Displacement caused by the Kumamoto Earthquake*

The study demonstrates the utilization of SAR interferometry technique for producing the damage assessment map. The primary objective of this study is to utilize the interferometric coherence from DInSAR processing, in order to obtain the insightful information of the damaged areas by the earthquake. The classification of non-urban and urban area was differentiated by pre-seismic coherence. Also, the threshold was estimated from the known urban areas to unknow areas. A greater value than 0.567 of the pre-seismic coherence was assigned to the urban class. The portion of damaged and non-damaged areas were evaluated by the normalized coherence change of co-seismic coherence. It shows the scale of damaged possibility from the light green to red color as shown in figure 4.

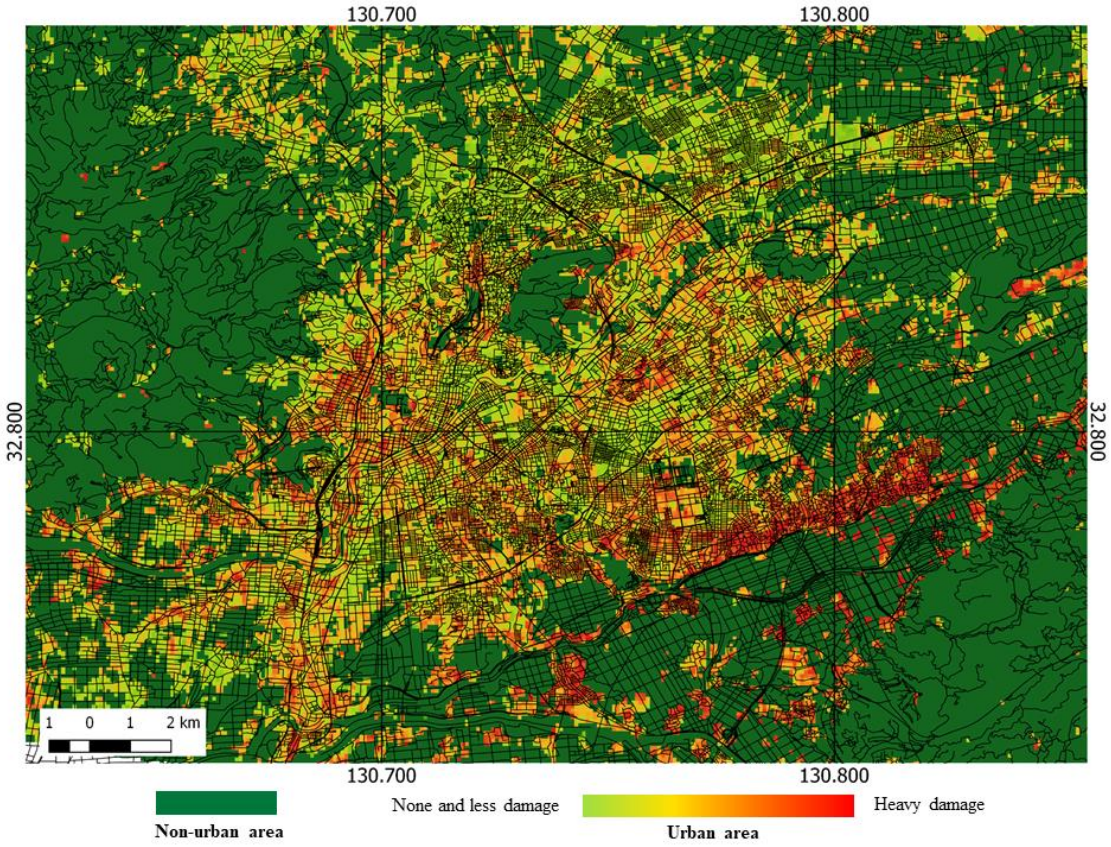

Figure 4: *The Damage Assessment Map Produced by the Multi-Temporal Sentinel-1A Images*

Table 1: *Statistical Information for Determining the Threshold of the Damage Assessment*

Statistical information	Mean	SD	Mean-3SD
Pre-seismic coherence identifies the urban areas	0.723	0.052	0.567
Coherence change identifies the damage areas	0.751	0.063	0.562

For accuracy assessment, the threshold between none to less damaged, and damaged area classes were defined by the known damaged areas and ground truth (Mashiki town is where earthquake caused the serious damaged buildings). Then, the value above 0.562 of ND was considered as damaged areas. The statistics and criteria are shown in table 1. The result map (figure 5) was classified into 3 main classes:

- Class 1- Non-urban area (Green)
- Class 2- None and less urban damaged area (Yellow)
- Class 3- Urban damaged area (Red)

The ground truth was taken from the combination of the survey, high-resolution satellite images and open street map (taken after the earthquake). The overall accuracy was outperformed to 88% compared to the ground truth using the confusion matrix as shown in table 2.

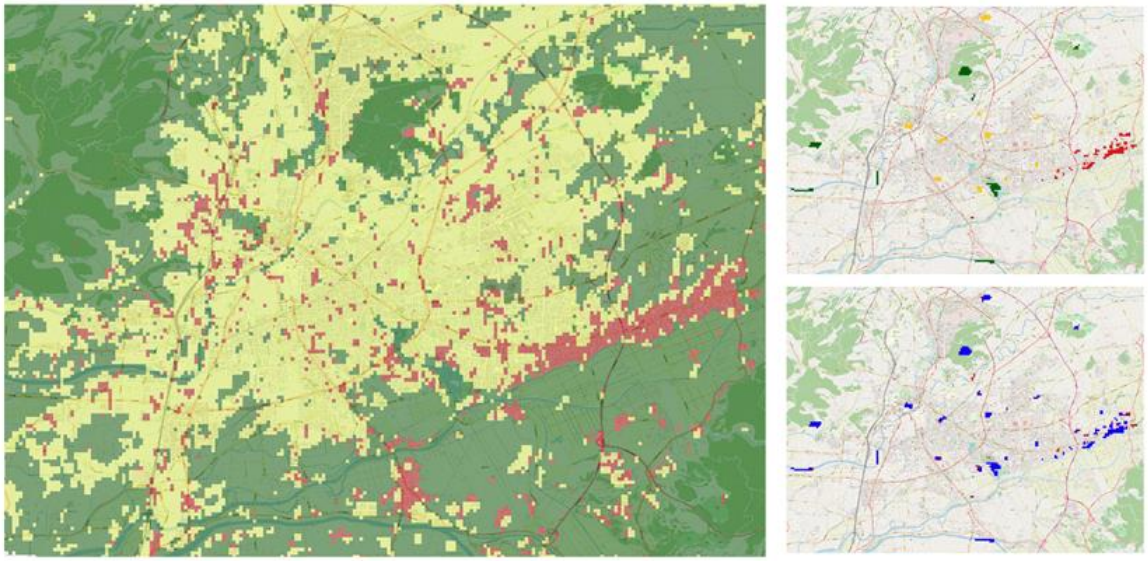

Figure 5: *The Left Image shows the Ground-Truth Data of Non-Urban (Green), None to Less Damaged (Yellow) and Damaged Area (Red). The Right Image Presents the Correct and Incorrect, which were shown in Blue and Red Color*

Table 2: *Accuracy Assessment (Pixels)*

Classes	Class 1	Class 2	Class 3	Sum	User's Accuracy
Class 1	135	8	0	143	0.94
Class 2	1	87	9	97	0.90
Class 3	7	18	103	128	0.80
Sum	143	113	112	**Overall accuracy is 88%**	
Producer's Accuracy	0.94	0.77	0.92	**Kappa coefficient is 0.82**	

Sentinel-1A could be appropriately applied in the earthquake damage detection. Also, the interferometric technique was efficient enough for detecting the earthquake displacement, and the damage assessment. The interferogram shows the phase change induced by earthquake from satellite looking dimension while the coherence analysis result presents the possibility of the large damaged areas without the interference of cloud coverage, which still performs the high accuracy. Moreover, the Sentinel-1A could provide the accelerated observation within 5 days after the disaster occurred. However, the further discussions are still concerned for the future study.

- The result was included some effects by the processing method and atmospheric conditions because Sentinel-1A provides C-band information. The wavelength is short about 5-6 centimeters, could have more effects than the longer wavelength.
- The spatial resolution was roughly generated with the default resolution at 100 meters operated by the software. It was rougher than using the higher resolution such as ALOS-2, which was investigated on the earthquake damage assessment (Tamkuan & Nagai, 2017). However, the spatial resolution depends on the SAR observation modes.
- For damage assessment, our study considered only the damaged, and none to less damaged areas. The multi-level of damages will be considered in further study.
- The spatial resolution is important for the damage classification. The density of urban and damaged areas could lead to the quality of the damage map. Some damaged buildings with 100x100 pixel of non-damaged areas may unfortunately be missing information. This point should be focused for next study to improve the accuracy for the earthquake detection.

4. Conclusion

This study proposed the method to detect the earthquake damaged areas using multi-temporal Sentinel-1A images. The damaged areas could be rapidly detected in the extensive area after only 5 days Kumamoto earthquake. The map was analyzed by the interferometric change of the images. The Interferometric pair of before-earthquake was used to determine the urban and non-urban areas. On the other hand, the after-earthquake pair (normalized change) was defined the urban damaged areas and none and less damaged of the urban areas. These classes were identified by known areas extending to all coverage, and computing by the statistical methods. The results were positively corresponding to our ground-truth data from the field survey. The overall accuracy was well-performed at 88% evaluating by the confusion matrix**.** Our method could expectedly support the geospatial analysis, and apply for unpredictable earthquake in the future.

References

Ansal, A. (2014). *Perspectives on European Earthquake Engineering and Seismology: Volume 1. Geotechnical, Geological and Earthquake Engineering* (Vol. 34).

https://doi.org/10.1007/978-3-319-07118-3

Arciniegas, G. A., Bijker, W., Kerle, N., & Tolpekin, V. A. (2007). Coherence- and amplitude-based analysis of seismogenic damage in Bam, Iran, using ENVISAT ASAR data. *IEEE Transactions on Geoscience and Remote Sensing*, *45*(6), 1571–1581. https://doi.org/10.1109/TGRS.2006.883149

Eguchi, R. T., Huyck, K., Adams, B. J., Mansouri, B., Houshmand, B., & Shinozuka, M. (2001). Resilient Disaster Response : Using Remote Sensing Technologies for Post-Earthquake Damage Detection. *Earthquake Engineering to Extreme Events (MCEER), Research Progress and Accomplishments*, 125–137.

ESA. (2012). Sentinel data policy and access to data. Retrieved January 3, 2019, from http://ec.europa.eu/DocsRoom/documents/648/attachments/1/translations/en/renditions/native

Hoffmann, J. (2007). Mapping damage during the Bam (Iran) earthquake using interferometric coherence. *International Journal of Remote Sensing*, *28*(6), 1199–1216. https://doi.org/10.1080/01431160600928567

Ishitsuka, K., Tsuji, T., & Matsuoka, T. (2013). Detection and mapping of soil liquefaction in the 2011 Tohoku earthquake using SAR interferometry. *Earth, Planets and Space*, *64*(12), 1267–1276. https://doi.org/10.5047/eps.2012.11.002

Konishi, T., & Suga, Y. (2018). Landslide detection using COSMO-SkyMed images : a case study of a landslide event on Kii Peninsula , Japan. *European Journal of Remote Sensing*, *51*(1), 205–221. https://doi.org/10.1080/22797254.2017.1418185

M. Ventayen, R. J. (2017). Multilingual Detection and Mapping of Emergency and Disaster-Related Tweets. *MATTER: International Journal of Science and Technology*, *3*(2), 240–249. https://doi.org/10.20319/mijst.2017.32.240249

Matsuoka, M., & Yamazaki, F. (2005). Building damage mapping of the 2003 Bam, Iran, earthquake using Envisat/ASAR intensity imagery. *Earthquake Spectra*, *21*(SUPPL. 1), 1–5. https://doi.org/10.1193/1.2101027

Miyazaki, H., Nagai, M., & Shibasaki, R. (2015). Reviews of Geospatial Information Technology and Collaborative Data Delivery for Disaster Risk Management. *ISPRS International Journal of Geo-Information*, *4*(4), 1936–1964. https://doi.org/10.3390/ijgi4041936

Mondini, A. C. (2017). Measures of spatial autocorrelation changes in multitemporal SAR

images for event landslides detection. *Remote Sensing*, *9*(6). https://doi.org/10.3390/rs9060554

Plank, S. (2014). Rapid Damage Assessment by Means of Multi-Temporal SAR — A Comprehensive Review and Outlook to Sentinel-1. *Remote Sensing*, *6*(6), 4870–4906. https://doi.org/10.3390/rs6064870

Raucoules, D., Ristori, B., de Michele, M., & Briole, P. (2010). Surface displacement of the Mw 7 Machaze earthquake (Mozambique): Complementary use of multiband InSAR and radar amplitude image correlation with elastic modelling. *Remote Sensing of Environment*, *114*(10), 2211–2218. https://doi.org/10.1016/j.rse.2010.04.023

Sandwell, D., Mellors, R., Tong, X., Wei, M., & Wessel, P. (2011). GMTSAR: An InSAR Processing System Based on Generic Mapping Tools. Retrieved May 15, 2014, from https://doi.org/10.2172/1090004

Sandwell, D., Mellors, R., Tong, X., Xu, X., Wei, M., & Wessel, P. (2016). GMTSAR: An InSAR Processing System Based on Generic Mapping Tools (Second Edition), 1–120.

Sandwell, D. T., Mellors, R., Xiaopeng, T., Matt, W., & Wessel, P. (2011). Open Radar Interferometry Software for Mapping Surface Deformation. *Eos*, *92*(2), 2011. https://doi.org/10.1029/2011EO280002

Stramondo, S., Moro, M., Tolomei, C., Cinti, F. R., & Doumaz, F. (2005). InSAR surface displacement field and fault modelling for the 2003 Bam earthquake (southeastern Iran). *Journal of Geodynamics*, *40*(2–3), 347–353. https://doi.org/10.1016/j.jog.2005.07.013

Suresh, D., & Yarrakula, K. (2018). InSAR based deformation mapping of earthquake using Sentinel 1A imagery. *Geocarto International*, 1–4. https://doi.org/10.1080/10106049.2018.1544289

Tamkuan, N., & Nagai, M. (2017). Fusion of Multi-Temporal Interferometric Coherence and Optical Image Data for the 2016 Kumamoto Earthquake Damage Assessment. *ISPRS International Journal of Geo-Information*, *6*(7), 188. https://doi.org/10.3390/ijgi6070188

Twele, A., Cao, W., Plank, S., & Martinis, S. (2016). Sentinel-1-based flood mapping: a fully automated processing chain. *International Journal of Remote Sensing*, *37*(13), 2990–3004. https://doi.org/10.1080/01431161.2016.1192304

Usman Kaoje, I., & Ishiaku, I. (2017). Urban Flood Vulnerability Mapping of Lagos, Nigeria. *MATTER: International Journal of Science and Technology*, *3*(1), 224–236. https://doi.org/10.20319/mijst.2017.s31.224236

Watanabe, M., Thapa, R. B., Ohsumi, T., Fujiwara, H., Yonezawa, C., Tomii, N., & Suzuki, S. (2016). Detection of damaged urban areas using interferometric SAR coherence change with PALSAR-2. *Earth, Planets and Space*, *68*(1), 131. https://doi.org/10.1186/s40623-016-0513-2

Yamazaki, F., & Matsuoka, M. (2007). Remote Sensing Technologies in Post-Disaster Damage Assessment. *Journal of Earthquake and Tsunami*, *01*(03), 193–210. https://doi.org/10.1142/S1793431107000122